Signal Processing 93 (2013) 2785–2803

Contents lists available at SciVerse ScienceDirect

Signal Processing

journal homepage: www.elsevier.com/locate/sigpro

Breast thermography from an image processing viewpoint: A survey

Tiago B. Borchartt [a,*], Aura Conci [a], Rita C.F. Lima [b], Roger Resmini [a], Angel Sanchez [c]

[a] VisualLab, Computer Institute, Federal Fluminense University, Sala 452 - 4 andar - Bloco D, Rua Passo da Pátria, 156 São Domingos, 24210-240 Niteroi-RJ, Brazil

[b] Department of Mechanical Engineering, Federal University of Pernambuco, Rua Acadêmico Hélio Ramos s/n, Cidade Universitária, 50740-530 Recife-PE, Brazil

[c] Department Ciencias de la Computación, Universidad Rey Juan Carlos, 28933 Móstoles-Madrid, Spain

ARTICLE INFO

Article history:
Received 10 February 2012
Received in revised form
1 June 2012
Accepted 16 August 2012
Available online 30 August 2012

Keywords:
Thermography
Infrared thermal imaging
Breast cancer detection
Computer vision
Pattern recognition
Computer aided detection/diagnosis (CAD)

ABSTRACT

Breast cancer is the leading cause of death among women. This fact justifies researches to reach early diagnosis, improving patients' life expectancy. Moreover, there are other pathologies, such as cysts and benign neoplasms that deserve investigation. In the last ten years, the infrared thermography has shown to be a promising technique to early diagnosis of breast pathologies. Works on this subject presented results that justify the thermography as a complementary exam to detect breast diseases. Several papers on the use of infrared imaging for breast screening can be found in the current medical literature. This survey explores and analyses these works in the light of their applications in computer vision. Consequently, the comments are organized according to the main steps of pattern recognition systems. These include: image acquisition protocols, exams storage, segmentation methods, feature extraction, classification or diagnostic and computer modelling. Main contributions of discussed papers are summarized in tables to provide a structured vision of the aspects involved in breast thermography.

1. Introduction

Breast cancer appears usually in the ducts, tubes that carry milk to the nipple, and lobules, glands that produce milk (Fig. 1). It occurs in both men and women, although male breast cancer is a rare disease. Some works have reported that the growth rate of a tumour is proportional to its temperature [1]. Screening looks for cancer before a person presents any symptom. It can help to find cancer at an early stage. When cancer is found earlier, the healing chances are greater. If a screening test result is abnormal, more diagnostic tests are necessary to define whether the finding is a cancer [2]. Each type of test presents specific characteristics. The combination of different explorations is fundamental, because most of them are complementary. For instance, information obtained from the breast ultrasound, dedicated breast CT, tomosynthesis and mammography are morphological. Thermography is a biological or a functional exam [1]. The infrared image presents physiological information of normal and abnormal functioning of the vascular system, sensorial and sympathetic nervous system, and inflammatory processes [3,4]. The concept of combined diagnostic, presented in the modern diagnostic centre, allows the achievement of a high degree of specificity and sensibility on such diagnosis [5].

Infrared images do not use ionizing radiation, venous access, or others invasive procedures. Besides these facts, it is painless and has no contact with the skin surface, causing no nuisance to the patient. It is low cost when compared to the traditional exams, such as mammography, ultrasound and magnetic resonance. It also has advantages for the diagnosis in young women, because dense tissues present difficulty for early visualization

* Corresponding author. Tel.: +55 21 2629 5479; fax: +55 21 2629 5627.
E-mail addresses: tbonini@ic.uff.br (T.B. Borchartt), aconci@ic.uff.br (A. Conci), rresmini@ic.uff.br (R.C.F. Lima), ritalima@ufpe.br (R. Resmini), angel.sanchez@urjc.es (A. Sanchez).

0165-1684/$ - see front matter © 2012 Elsevier B.V. All rights reserved.
http://dx.doi.org/10.1016/j.sigpro.2012.08.012

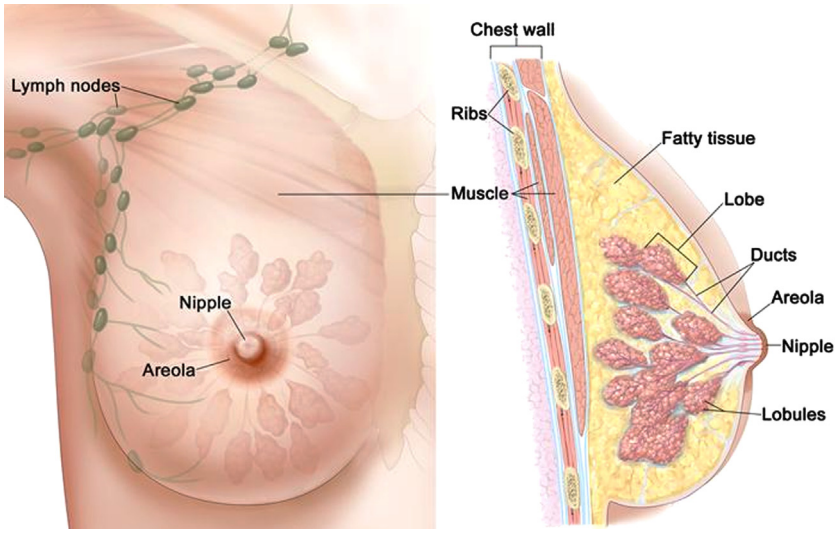

Fig. 1. Anatomy of the breast.

of problems by X-ray. For instance, micro calcifications and masses are usually well visible only in mammograms of women in non reproductive ages [6]. Moreover, thermography is very useful for detecting non palpable breast cancer; that is, those that cannot be detected by other exams. This also applies to non palpable but histological advanced or those with fast and aggressive growth [3].

Signal and image processing techniques have been successfully applied on medical data as a tool for screening and improving diagnosis. However, it is not easy to find papers containing a critical analysis of works on thermal images of breasts. Keyserlingk et al. [7] consider the use of infrared (IR) imaging to aid on the diagnosis of clinical exams from the latest 1960s. During the 1970s they showed that the combination between thermography and mammography increased the sensitivity of cancer detection in approximately 10% [7]. In the last two decades, the breast thermography has achieved an average sensitivity and specificity around 90% for breast tumour detection [8]. An abnormal thermogram may indicate significant biological risk for the existence or for the development of breast tumours [9]. Studies showed that a thermogram could identify precancerous or cancerous disease earlier than others exams [1,3]. Some authors state that the thermography may have the potential to detect breast cancer up to 10 years earlier than the traditionally golden method: the mammography [8,10,11]. Moreover, every time the breast is exposed to X-ray, the cancer risk increase by 2%, and the premenopausal breast is highly sensitive to radiation [12].

This paper presents a review on recent image processing works related to the thermography for breast diseases detection and diagnosis. A special attention is given to the early detection of cancer, since it is the most serious breast pathology and the most frequent neoplasm in women [5]. Evaluating the use of thermography in a cancer detection program is not the aim of this review. This survey is organized as follow. An initial section about thermography (Section 2) is followed by sections on works and techniques used in the main stages of a computer aided detection or diagnosis (CAD) systems. The first step in CAD systems is the acquisition and storage of images. Several acquisition protocols of breast thermal images and ways for storing these images are described in the literature, but there is no standard for this (Section 3). The thermograms are usually acquired in a larger area, which makes necessary the use of segmentation techniques for region of interest (ROI) extraction (Section 4). Other important steps in a CAD are the choice of features extracted from the ROIs (Section 5), and their classifications (Section 6). There are also two additional sections, one about the interpretation of thermal images in the diagnosis of pathologies (Section 7) and other about computer simulation or modelling (Section 8). Finally, the conclusions of this survey work are summarized in Section 9. Whenever possible, the revised papers are presented in chronological order to allow a better comprehension of the evolution of techniques used in each section.

2. Thermal breast imaging

Although there are thermal images obtained by contact, the type considered here are those named thermograms. The human body emits infrared electromagnetic radiation. The thermographic camera is sensitive to this kind of radiation. The images acquired by this camera are formally denominated telethermography or telethermometry [13]. Its sensors capture the natural thermal radiation generated by an object at a temperature above absolute zero [14]. All objects that have temperatures above this value (that is 0 K or $-273\ ^{\circ}C$) emit infrared radiation from its surface [8]. The relationship between the energy radiated by an object and its temperature is described by the Stefan–Boltzmann law [15]. The measured infrared radiation emitted by one point of the skin can be converted directly into a temperature value that

represents this point and then mapped to a pixel in a false-color image of the scene.

Thermal sensor used to capture infrared radiation varies with the type of camera. Usually, the camera used for biomedical proposes has sensors whose sensitivity is around 0.05 °C and a range of capture that varies from 15° C to 45 °C. The generated images have a minimum resolution of 320×240 pixels. The appropriate image dimensions can vary with respect to the distance of the patient to the camera. The camera estimates the human body temperature based on three emitted components: the radiation of the body, the radiation of the objects that are in the neighbourhood and that is reflected by the body, and radiation of the surrounding medium. Some parameters must be set at the camera so that it can estimate the influence of radiation of the medium where the images are obtained. These parameters are: emissivity of the human body (that is around 0.98), environmental temperature, relative humidity, temperature range of operation and distance between the camera and the body. The camera converts the measured radiation by its sensor to a matrix with temperature values. Skin radiance is an exponential function of the surface temperature, which in turn is an indicator of the level of blood perfusion inside the body. Changes in the blood perfusion may occur by a variety of reasons, such as inflammation, angiogenesis, and previous traumas [16,17].

Biomedical applications are especially concerned to the measured temperature distribution, which is intrinsically connected to biological and physiological processes related to some disease. Breast cancer cells produce nitric oxide (NO) [18], it interferes with the normal neuronal control of the blood vessel flow and causes a local vasodilatation in the early stages of cancerous growth enhancing the angiogenesis in later stages [19,20]. Subsequent increased blood flow in the area causes a temperature increase compared to the normal breast temperature. Even deep breast lesions seem to have the ability to induce changes in the skin temperature [21]. Breast cancer metabolic processes may also contribute to the detectable heat increase. It is believed that in healthy individuals, the temperature is generally symmetrical across the midline of the body [22,17]. Subjective interpretation of many diagnostic imaging modalities, including infrared thermographic images, relies on the underlying philosophy that normal contralateral images are relatively symmetrical, and that asymmetries may indicate any abnormality [23]. Therefore, IR thermography can detect a breast disease by identifying areas of asymmetric temperature distribution on the breast surface [24–26]. These asymmetric temperature distributions are often associated with physiologic changes, as well as the development of neoangiogenesis. Much of the past and current uses of this technology have performed measurements that assessed the differences when comparing both breasts [3]. Asymmetry between the breasts is one of the most important signs that can be measured and quantified [1]. Determination of areas within the breasts that show a high level of blood perfusion, or vessels are also of great importance. It is well known that hot and cold spots are strong indicators of an underlying dysfunction [27]. Most of the time, the thermogram interpretation is based on exaggerate vascularisation, hot spots and on asymmetries between breasts [23].

In numerical simulations, heat transfer in the breast tissues was modelled by Pennes' equation [28,29]. IR images can be displayed in grey scale or in false-colour by many types of palettes, depending on the camera or software used. The number of colours and the RGB values of each colour differ according to used palette. Temperature associated to each point of breast surface can be applied in analysis and in detection of different kinds of diseases. In conclusion, these aspects must be examined to reveal functional behaviour in the case of normal or abnormal heat distribution [30].

3. Thermal image acquisition and storage

Thermograms are sensitive to environmental changes in temperature, humidity and air flow. As a result, they need to be captured under strict protocols. A major factor related to the inconsistency of works in the breast thermography is the several protocols under which the acquisition procedures are performed. Be able to provide a database public and available to all researchers interested in such issue and a discussion about the use of a unique protocol of capture are, perhaps, the most important goals on the use of IR images in visual computing, artificial intelligence applications and Computer Aided Detection and Diagnosis (CAD) systems.

In this section, papers that describe acquisition protocols and IR image storage techniques are reviewed, and two tables are presented. Table 1 shows a collection of image acquisition protocols described in the literature, and Table 2 presents a relation of some data used in the revised works.

3.1. Acquisition protocols

The thermal image acquisition can be categorized with respect to the body behaviour under the heat transfer as *static* or *dynamic*, and also categorized according to the repetition as *single*, *sequential* or *accompanied* capture. In static acquisition, the patient is in thermal equilibrium with the environment. Dynamic acquisition is applied in monitoring the recovery of the skin temperature after a caused thermal stress (e.g., cooling or heating) or chemical stress (e.g., vasodilatations or vasoconstrictions). In single acquisition, images of the patient are captured in an instant of time. This kind of acquisition is suitable for identifying hot and cold spots areas and for measuring the asymmetries on the skin temperature distribution [31]. In the sequential mode, a series of images are acquired sequentially over a period of minutes, which can be set in the camera, previously. In the accompanied mode of capture, acquired images are separated by a substantial time interval (each 3 or 6 months) in order to monitor the progress of some disease or to detect it earlier [31].

When a dynamic capture procedure is performed to evaluate a thermal stress, the patient is exposed to a cool airflow directed to her breast and images are acquired

Table 1
Summary of the acquisition protocols.

Paper	Type of acquisition	Room temperature	Special recommendations before capture
Koay et al. [48]	Single/dynamic: the breast area was cooled slightly with a fan for approximately 20 min	22 °C	For data collection, the patient was asked to avoid alcohol, caffeine, pain medication, lotions, and stop smoking two hours before the test
Ng and Kee [43]	Single/static: 20 min to stabilize	20 to 22 °C and humidity of 60	Reduction of heat fonts during acquisition. Patient recommendations of no use of alcohol, cigarettes, skin products
Arora et al. [32]	Sequential/dynamic: 4 min in a cold air directed at the breast	Not cited in the paper	Not mentioned
Bezerra [45], Silveira Filho et al. [59], Araujo et al. [34], Motta [35]	Single/static: 10 min	25 to 28 °C	Without special recommendations.
Agostini et al, [13]	Sequential/dynamic: 50 frames/s to 200 frames/s	Not cited in the paper	Not mentioned
Acharya et al. [44]	Single/static: 15 min to stabilize	20 to 22 °C (within ± 0.1 °C), and humidity was maintained at 60% $\pm$ 5%	Not mentioned
Delgado and Luna [39]	Single/static: 15 min to stabilize	18 to 23 °C	Not mentioned
Kapoor and Prasad [33]	Single/dynamic: 7 to 10 min in a directed cold air at the breast	22 °C	Capture in a dark room for minimum interference
Amri et al. [37]	Single/static: 10 to 20 min to stabilize	18 to 22 °C	Patient recommendations of no use of alcohol consumption, physical exercises, skin products
Kontos et al. [40]	Single/static: 10 to 15 min to stabilize	22 °C	Not mentioned
Wishart et al. [6]	Sequential/dynamic: 5 min in a cold air directed at the breast	Not mentioned	Not mentioned
ACCT [41]	Accompanied/static	Not mentioned	Not mentioned

Table 2
Summary of the number of acquisition and database used.

Paper	Number of captures per patient	Public database/ number of patients	Dedicated equipment for positioning	Patients signed an informed consent about their images use
Koay et al. [48]	Not specified	No, 19 patients	No	Not mentioned
Ng and Kee [43]	3 images: 1 frontal, 2 lateral	No, 90 patients	No	Not mentioned
Arora et al. [32]	100 frontal images per patient	No, 92 patients	Yes: sentinel BreastScan	Yes
Tang et al. [49]	Not mentioned	No, 117 patients	Yes: TSI thermographic system	Not mentioned
Agostini et al. [13]	Movie in frontal position	Not cited in the paper	Yes: examination table with the backrest inclination of 40°	Yes
Bezerra [45], Araujo et al. [34], Silveira Filho et al. [59], Conci et al. [61–63] and Silva [112].	8 images: 4 frontal, 4 lateral	Yes, 220 patients	No	Yes
Delgado and Luna [39]	3 images: 1 frontal, 2 lateral	Not mentioned	No	Not mentioned
Antonini et al. [38]	5 images: 1 frontal, 4 lateral	No, 3 patients	No	Yes
Kontos et al. [40]	3 images: 1 frontal, 2 lateral	No, 63 patients	Yes: backless chair with rotation	Yes
Wishart et al. [6]	250 images per patient	No, 100 patients	Yes: Sentinel BreastScan	Yes

during or after the exposure [5,32,33]. The examination procedure proposed by Arora et al. [32] takes about 4 min per patient, and the dynamic sequential acquisition produces more than 100 thermal images during administration of a cold stress. Registration of images in time is assisted by three markers on the patient skin. In the single dynamic acquisition used by Tejerina [5] and Kapoor and Prasad [33], the breasts are cooled slightly for 7 to 10 min, just before image capture. The recommended room temperature for this procedure is of approximately 22 °C, and the room must be darkened during the test in order to minimize the interference from other infrared sources. The controlled room temperature condition is intended to ensure that, the heat loss due to evaporation may be neglected. Severity of room temperature and the adaption time to room temperature when thermography is used for

screening test was investigated by Usuki et al. [23]. In dynamic acquisition with cold stress protocols, skin temperature pattern is regarded as a balance between heat conduction from deeper vessels and tissues, and heat loss by air convection and radiation at the surface. Besides image capture, some interest aspects must be registered, such as patient age and date of the first day of last menstrual period, because hormonal fluctuations are related to temperature variations and they could affect the stability of thermographic measurements [22].

In single static acquisition protocols, patients spend from 10 to 20 min for acclimatization before image acquisition [34–40]. Most of the works suggested that the room must have a controlled temperature in the range of 18C to 22 °C and humidity about 60%. However, there is case where images are acquired in tropical climate region (25 °C to 28 °C), when conditions of temperature and humidity are registered, but not controlled [36].

In the American College of Clinical Thermology (ACCT) [41] protocol, patients are partially disrobed, and the medical history is taken. The first acquisition is called *thermal signature*, and it is used to compare with other thermograms from the same patient. Patients are required to take a new thermogram after 3 months (static accompanied protocol).

An alternative acquisition protocol was tested by Agostini et al. [13]. The proposed protocol aims to observe the influence of skin temperature fluctuation and blood perfusion. The authors acquire a sequence of consecutive thermal images with rate ranging from 50 to 200 frames/s. Then they use the frequency domain of the small temperature fluctuation in the breast area, rather than considering the classical static skin temperature. Each sequence is comprised of 500 thermal images with dynamic range of 14 bits and 256×256 pixels.

On the day of acquisition, patients are ideally required to avoid other controllable factors that could potentially to produce effects on the skin temperature such as alcohol consumption, physical exercise and application of cosmetic preparations on the breast surface [42,43]. Kapoor and Prasad [33] recommend their patients to avoid alcohol, caffeine, stop smoking two hours before the test, and do not apply lotions on the body area to be imaged. Ng and Kee [43] also instruct their patients to abstain from any physical activities for 20 min before the exam to reduce the body metabolism and stabilize the body temperature. Acharya et al. [44] consider patients within the period of the 5th to 12th and 21st day after menstrual cycle.

3.2. Positions and number of captured images

A universally accepted acquisition protocol was not defined for thermal imaging yet. As a result, each clinic and hospital acquires a different number of images in each acquisition section and assumes different patient positions in relation to the camera. Agostini et al. [13] use only one frontal image per patient with their arm up and hands resting over their heads. Tejerina [5] uses at least three positions: (i) frontal with hands on the head; (ii) external lateral of the right breast, and internal lateral of the left breast; and (iii) external lateral of the left breast and internal lateral of the right breast. Delgado and Luna [39] use a static protocol where three thermal images are acquired: (i) frontal; (ii) left oblique; and (iii) right oblique. The static protocol described by Antonini et al. [38] defines five capture positions: (i) frontal, (ii) right semi-oblique; (iii) left semi-oblique; (iv) right oblique; and (v) left oblique. Three images were obtained from each patient by Kontos et al. [40]: (i) frontal; (ii) the left and (iii) the right oblique at 45° to the midline to exposure all aspects of the breasts. During the examination, the patients of Ng and Kee [43] are required to take off the top clothing and their hands are positioned behind their heads, then three thermograms are taken: one frontal and two lateral. A minimum of eight images per patient: (i) frontal, with arms lowered and hands on the hips; (ii) frontal, with hands on the head; (iii) only the right breast; (iv) only the left breast; (v) external lateral of the right breast; (vi) external lateral of the left breast; (vii) internal lateral of the right breast; and (viii) internal lateral of the left breast are acquired by some works [35,45–47].

3.3. Cameras and acquisition systems

Ng and Kee [43] collected breast thermograms of 90 patients in Singapore General Hospital using a thermal camera Avio TVS-2000 MkII ST. Arora et al. [32] uses the Sentinel BreastScan™ (Infrared Sciences Corp.). During the exam the patient sits on a chair disrobed from the waist up, with her arms on the armrests. Once the exam begins, the patient's thermal images are being recorded for analysis. A few seconds later a cool air flow is turned on. The examination lasts approximately 3 to 4 min. The system searches for signs of abnormal angiogenesis, as well as asymmetric thermal indicators. Analysis takes approximately 4 to 5 min and a report is generated. Tang et al. [49] considers 117 patients from the People's Liberation Army General Hospital (PLAGH), China. Images were acquired using the TSI-21 Thermographic System [50]. These images were of 256×256 pixels, 47 with malignant tumours and 70 with benign cases. In the Agostini et al. [13] acquisition, the patients were asked to lie down onto an examination table with backrest inclination of 40° from the horizontal plane. The optical axis of the infrared camera was perpendicular to the backrest of the examination table. The camera was placed at a distance of 220 cm from patient. The authors used one AIM256Q camera produced by AEG infrarot-Module GmbH, having a noise equivalent temperature difference (NETD) equal to 17.3 mK at 300 K, with an interpolation time equal to 20 ms. Wishart et al. [6] have studied the performance of IR in 100 women prior to their breast core biopsy. They used Sentinel BreastScan apparatus. Four different models of this system of examination are compared: screening, neural networks, manual by experts and an artificial intelligence method that the authors call NoTouch BreastScan. Comparisons are separated by ages (under 50, 50–70 and over 70) and consider sensitivity and specificity. The study was carried out from June 2007 to January 2009 with patients from the Addenbrooke's

Hospital, Cambridge, UK. All patients signed a consent term. Images were taken with patients disrobed to the waist and appropriately positioned in an ergonomic chair with arms supported at eye level. Nurhayati et al. [51] present a research performed at the Yogyakarta Hospital in which 150 women were examined. Digital thermal camera Fluke was used for thermogram acquisition. Three groups, each one with 50 patients was then assigned, consisted of healthy, chemotherapy and advanced group. Kontos et al. [40] considered a total of 126 breasts examined of 63 patients (58 women and 5 men). The average age of patients was 47.6 (between 26 and 82 years). Cancerous lesions were diagnosed in 20 breasts. Before taking the examination the patients signed a consent term allowing their thermal images were used in studies. Patients were instructed to sit on a backless chair with rotation with their hands on the top of their head. The thermographic camera was positioned at 1 m from the chair. The Meditherm med2000 thermal imaging system [52] was used for the thermographic imaging. The works of the PROENG project [36] acquire images from patient of the University Hospital of the UFPE (Brazil). More than 220 patients were examined until 2011 by use of a Flir ThermaCAM S45 [55] in 320×240 pixels [34,35,45–47,53,54].

3.4. Public available databases

Storage of IR breast thermal images in databases and their categorization could contribute to advance the state of art in the analysis of thermograms. Such databases could support specialists and students in diagnostic decisions providing both educational and research activities. They could also be analysed by Artificial Intelligence and Data Mining algorithms for machine learning purposes. Unfortunately, in contrast to other types of medical images (e.g., mammography, ultrasound or magnetic resonance), there is no expressive public database in digital infrared thermal images as the Digital Database for Screening Mammography (DDSM) or Mammographic Image Analysis Society (MIAS) [56]. Thermograms have been stored mainly in private image database, available only to internal diagnosis proposes [5,57], and mostly of the time only the patient and his physician could access the images. Maintenance of a public database available for all interested researchers is of great importance to improve the possibilities of research in the area.

Koay et al. [48] developed a study where they have used thermal images of 19 patients selected from a total of 86 images acquired in 1984 by the team of the Moncton Hospital. From these images, 14 were from patients without any pathology and 5 were from patients with pathology. The works of Bezerra [45] and Araújo et al. [34] describe a public available database [58]. Thermograms can be accessed by searching for specific unique identifiers, such as the number of IR acquisition or the patient's medical record number. Image search can be done also for more general fields, such as age, type of capture, patient diagnosis or exam date. Thermograms stored in this database have been taken from patients of the University Hospital of UFPE (Brazil) or from volunteers that have signed a consent form allowing the use of their images [36]. The acquisition and storage of images were approved by Ethical Committee of UFPE and registered at Brazilian Ministry of Health; all patients signed a consent term allowing the publication in the database and free use of their images. Silveira Filho et al. [59], Serrano et al. [60], Motta [35], Motta et al. [47], Viana et al. [46], Conci et al. [61–63] and Borchartt et al. [54,64] use this database. Motta et al. [47] present a subset of this database, which includes some ground true of ROI segmentations performed by specialists [36].

4. Pre-processing, segmentation and ROI extraction

Segmentation of ROI intends to separate the main parts of the rest of the image. The breast is made up of connective tissue, fat, lobes and ducts. Each breast also presents blood and lymph vessels. Lymph nodes filter substances present in the lymph and help fight against infections and diseases. Clusters of lymph nodes are found in the axillar region (that is under the arm), above the collarbone, and chest. The ROI extracted from the acquired images must include all breast tissues and the near ganglion groups related as much as possible. Some medical suggest the inclusion of half of the arm in it. About 75% of lymph from the breasts drains into the axillar lymph nodes, making them important to the diagnosis of breast cancer. Fig. 1 shows the lymphatic system of the mamma near the throat (or neck) and the axillar glands. Extraction of the region of interest (ROI) limits based on the IR images is a challenging task due to the amorphous nature and the lack of clear limits in these images [65]. Due to the difficulty in developing fully automatic systems, most authors prefer the manual or semi-automatic ROI extraction.

Lipari and Head [66] proposed an algorithm of semi-automatic segmentation where each breast is divided into four quadrants. Four reference points, informed by the user, divide the breasts: the chin, the left side, the right side and the bottom edge of the breast. Each of these points connected to the nipple separates the image into four distinct quadrants.

Herry and Frize [67] performed statistical analysis and compare the intensity distribution on both breasts. From such an analysis they extract the contours using a simple contour detector and morphological operations. However, the authors state that the initial segmentation may be done manually.

Zhou et al. [65] proposed the use of an automatic algorithm based on Level Set Method (LSM) to extract the edges of an object in a thermal image. The proposed approach is based on direction and magnitude of edge pixels. An edge map represents the gradient magnitude and direction. Linear and isotropic features based on Gaussian filter are used to obtain this edge map. Three or four randomly selected points within the ROI (or on its edge) are used as initial points. Initial pixels localize the place where the evolution of the method begins and provide information about the gradient.

The segmentation procedure proposed by Scales et al. [68] is comprised of eight steps: (i) manual removal of body borders (as shoulders and waist); (ii) contour detection by using Canny edge detectors; (iii) elimination of left and right body limits; (iv) use of two approaches: Hough transform (HT) and connected components for improving detection of the lower border; (v) interpolation of detected border by curves; (vi) detection of region with greatest curvature in left and right sides of the body; (vii) estimation of breast upper limit using empirical rules; and (viii) isolation of ROI based on the frontiers found in previews steps. The authors report that only 4 from a set of 21 images presented satisfactory ROI detection results when the HT-based approach was applied. From the poor results, 12 of them were due to detection of the inframammary fold and, for the other ones, the error was attributed to the bad edge detection. The connected edge detection-based algorithm achieved successful segmentation in 13 of 21 images. Moreover, 2 of the 8 unsuccessful detections could become satisfactory if the parameters of the edge detection scheme were set manually [68]. Additionally, another image would become satisfactory if a larger neighbourhood is used in detection of connected pixels.

Qi et al. [69] applied segmentation techniques based on edge detection. They noticed that the use of a naïve edge detection scheme would result in several undesired curves inside body region. Since the inframammary fold has an almost parabolic shape, the intra-body detection issue is overcome by using a parabolic HT. Body borders were identified using three limits: (i) axillar, obtained from the points of greatest curvature; (ii) breast border, from the found HT parabola; and (iii) central point, from the intersection point of the HT parabolas. Some characteristics may be observed in their result, such as lost of some breast area, and ROI's lack of symmetry. The first drawback may discard regions with possible lesion, and the second might disturb some automatic diagnosis methods based on comparison of mirrored regions. Besides the technique not be fully automatic, it is possible to see the disparity in the size of each breast obtained. These, as mentioned before, could be undesirable for CAD systems based on comparisons of corresponding parts.

Jin-Yu et al. [70] presented a genetic algorithm based on chaotic two-dimensional Otsu method [71]. This algorithm can be used in generic IR thermal images, not only in breast thermograms. The proposed method was designed to segment regions with higher temperatures in thermal images presenting high levels of noise. It is comprised of four steps: (i) use logistic mapping equations to initialize the population of the genetic algorithm; (ii) use the chaotic two-dimensional Otsu method [71] to calculate fitness of current population; (iii) when the end condition is achieved, the best individual is returned and the algorithm ends, otherwise the procedure continues; (iv) generate a new population by selection, crossover and mutation operations and return to step (iii). Each individual of the population represent a possible ROI segmentation. Authors report that average time of the segmentation to 10 thermograms with dimensions of 198×173 pixels is 4.83 s.

Schaefer et al. [72] used statistical methods and fuzzy classification to diagnose breast cancer, but their ROI's segmentation was done manually by experts.

Kapoor and Prasad [33] proposed an automatic segmentation technique composed by two main steps. In the first step, a Canny edge detector to extract the lateral boundaries of breast is used. The second step uses a HT to extract lower breast boundaries.

Motta et al. [47] presented a fully automatic segmentation method. Such method is based on automatic threshold, automatic border detection, and extraction of inframammary folds by using mathematical morphology and cubic-spline interpolation. The described approach separates both breasts as much symmetrically as possible. There are two drawbacks in this method of automatic ROI extraction. The first is that the detected ROI's upper limit (i.e., the lower line crossing the axilla) may exclude a portion of the upper quadrant of the breast. The second drawback is not including the lymphatic nodes of the mamma in the axillar regions (see Fig. 1). Although both regions may present cancer, the second is usually neglected by automatic segmentation techniques.

Motta [35] also improves a previous approach [47]. The new method has 7 main steps: (i) a threshold is used to detect the inframammary fold which is considered as ROI lower limit; (ii) Otsu's method [71] is employed to remove the background; (iii) ROI upper limit is obtained by detecting the axilla; (iv) arms and external objects are removed by detecting the largest object in the image; (v) body central axis is used to separate the breast; (vi) inframammary fold is found; and (vii) a vertical displacement is performed to make each ROI more adequate for feature extraction based on the symmetrical analysis. Motta [35] applied his approach to 150 patients and compared them to manual (Ground true) segmentations performed by 5 specialists. The resulting ROI's are available for public comparison [36]. Such automatic results were evaluated qualitatively and quantitatively considering the rates of false positives, false negatives, true positives and true negatives.

Kafieh and Rabbani [73] presented a wavelet-based denoising method for breast infrared images. They model the noise variance as a function of the image intensity and use a wavelet-based maximum a posteriori estimator for noise removal. An interesting aspect of this paper is a review of other 10 works concerning noise removal in IR images.

Zadeh et al. [74] used a parabolic HT for ROI segmentation. For this purpose, edges are detected through a logarithmic method. Unfortunately, initial results of the edge detection are contaminated with high rates of noise. As a consequence, the computational cost of HT becomes higher. In order to avoid this issue, the authors apply a 6×6 Gaussian filter for noise reduction.

Borchartt et al. [54] use a segmentation method proposed by Motta [35]. They calculate the performance of Motta methods. On average, the total processing time for ROI extraction was 36.63 s. However, more than 96% of this time is due to the execution of the HT algorithm (35.17 s). The maximum total time obtained was 83 s, where 82 s was expended only in achievement of HT. The

Table 3
Summary of segmentation and ROI details of revised articles.

Paper	Degree of automation[a]	Region included[b]	Validation
Lipari and Head [66]	1	LN	Not specified
Herry and Frize [67]	0	P	Not specified
Zhou et al. [65]	2	P	Compare with other simple method of edge detection
Scales et al. [68]	1	P	2 approaches for segmentation are presented and compared
Ng and Kee [43]	0	P	Not specified
Qi et al. [69]	2	P	Not specified
Jin-Yu et al. [70]	2	P	Not specified
Schaefer et al. [72]	0	P	Medical experts made the segmentation
Kapoor and Prasad [33]	2	P	Not specified
Motta [35], Motta et al. [47] and Borchartt et al. [54]	2	P	The images were manually segmented by five experts to compare the results
Zadeh et al. [74]	2	P	Not specified

[a] Degree of automation: 0—manual; 1—semi-automatic; 2—fully automatic.
[b] Region included: P—primary breast region; LN—lymph nodes region.

minimum total time for ROI extraction is 8 s, where 7 were spent only in the HT algorithm. Table 3 summarizes the different segmentation and ROI extraction approaches commented.

5. Feature extraction

Compared to other types of medical imaging, thermography has a very low cost. On the other hand, it presents some disadvantages that are not common to other early cancer detection methods, such as (i) its relatively low sensitivity for deep and small tumours, (ii) its inability to distinguish tumours from other "hot spots" like local inflammation, and (iii) subjectivity used by physicians while interpret IR images for diagnostic purposes [16]. Computer vision and pattern recognition techniques may overcome those disadvantages. The first steps toward using these techniques are related to choosing characteristics that will be extracted from the IR images in order to compose a feature vector, and how to compare such vectors. This section presents a chronologic review on works related to feature extraction and comparison of breast thermal images.

Lipari and Head [66] considered asymmetry between breasts and quadrants. The features extracted are: mean, median, standard deviation, maximum and minimum value of temperature for each breast and each quadrant. The paper does not present any results in sensibility or specificity, only some comparisons between values of features extracted from each breast and quadrant.

Kuruganti and Qi [27] segmented each breast in thermal images using generalized HT to extract parabolic curves defining the lower part of the breast. In turn, the following features are extracted from the histogram of each breast region: four moments (mean, variance, skewness and kurtosis) and entropy measures. They used 6 normal thermograms and 18 cancerous thermograms to validate the proposed classification scheme. The authors observe that the high-order statistics (skewness and kurtosis) are the most effective features to measure asymmetry, while low-order statistics and entropy do not assist in detection of asymmetries. For testing their methodology, the authors have used the correlation measure to asymmetric analysis. From the set of features derived from the testing images, the existence of asymmetry is verified by computing the ratio of feature of left to the right ROI.

Koay et al. [48] extract 10 features from thermal image for each quadrant of each breast. Quadrants are defined having the nipple as a common point. Extracted features are: mean temperature difference, standard deviation difference, median, maximum, minimum, skewness, kurtosis, entropy, area and heat content. After feature extraction, the authors use the SPSS statistical software to determine the correlation among the features. Five features are highly correlated: mean temperature difference, standard deviation difference, skewness, kurtosis and heat content [48].

Ng and Kee [43] analyse 82 patients, where 30 of them are asymptomatic patients (aged 51 ± 8), 48 patients have benign breast abnormality (aged 46 ± 10), and 4 patients developed cancer at least on one breast (aged 45 ± 5). The authors estimate the temperature of each breast points and compute median, modal and mean temperature of the breast. They also consider in the analysis other characteristics (such as age, family history on breast cancer, hormone replacement therapy, presence of palpable lump, age of menarche, previous breast surgery or biopsy, presence of nipple discharge, pain in the breast, menopause over 50 years, and first child over 30 years of age).

Qi et al. [69] describe two methods for IR diagnosis of breast diseases. The first is based on the thermal histogram of patients posterized in ten levels of grey. From these histograms the *k*-means algorithm is used to decide if the patients are "with disease" or "health". The *k*-means algorithm builds clusters for possible classifications, and it considers the distance from set of characteristics to the centroid of the clusters for decision. The second method presented by Qi et al. [69] uses mean, variance, skewness, kurtosis, correlation, entropy and joint entropy as characteristics for composition of a feature vector. They suggest that the classification using these features should be made through the algorithm of *k*-nearest-neighbour

(KNN). However, they do not present the evaluation results, only the extracted features.

Tang et al. [49] propose the analysis of what they named localized surface temperature increases (LTI) from thermal breast images. The LTI is showed as spot or vascular pattern in the thermograms. They propose a two-step process to realize the cancer detection: (i) the visual finding of suspicious focus in breast, and (ii) the measure of the LTI amplitude [49].

Schaefer et al. [75] proposed an application of content-based image retrieval (CBIR) to thermal medical images. CBIR allows the retrieval of similar images based on features directly extracted from the image data. These features are then stored alongside the image and words. The authors use two-dimensional Cartesian moments and each thermal image is thus characterised by its four first moment invariants.

Wiecek et al. [76] suggest as features statistical parameters of the first order (i.e., obtained without considering the neighbourhood), characteristics based on histogram, and the second order features (i.e., considering the location of pixels) from the matrix of co-occurrences. The used first-order parameters are: mean temperature, standard deviation, variance, skewness and kurtosis measure. The second-order measures are: energy, variance, difference variance, correlation, inverse difference and entropy.

Schaefer et al. [72,77] build a feature vector with 38 features. The first four features are ROI's basic statistical features, namely the absolute difference of the mean temperature, the standard deviation, the median temperature and the 90-percentile of left and right breast. Other four are based on image moments: absolute difference between the ROI centre of gravity, geometric centre, and the first moments (m_{01} and m_{10}). Some of the used features are from the normalized histogram of both ROIs: the cross-correlation between the two histograms, the absolute value of the maximum difference histogram, the number of bins of the difference histogram exceeding an empirically chosen threshold, the number of zero crossings, the energy and the difference of the positive and negative parts of the histogram. Other eight features are derived from cross co-occurrence matrix: homogeneity, energy, contrast, symmetry, and the first four moments. One element of their feature vector is computed as the sum of each breast's entropy and the joint entropy. Two features came from the Fourier spectrum: the maximum difference of the values of the spectrum and the maximum distance this position of spectrum to the centre of the graphic. After application of Laplacian filter to enhance image contrast, the authors extract nine more Fourier transform-based features: the mutual information and the eight features of cross co-occurrence matrix.

Silveira Filho et al. [59] assessed the image texture using a gliding box algorithm considering the image lacunarity measures [78,79]. They show that lacunarity can be used to distinguish between thermal images of patient with or without pathology. Serrano et al. [60] and Conci et al. [63,80] improve the method developed by Silveira Filho et al. [59] and extracted a total of 133 features, where 36 of them are Hurst coefficients and 97 features are from lacunarity. Hurst coefficient is a fractal dimension that is related to density, in other words, how much the image or object occupies the space that contains it. For texture feature extraction by Hurst coefficient, the authors compute mean and standard deviation using the right and left breasts, and subtraction of both through a movable windows varying among 5, 7, 9, 11, 13 and 15 pixels. The lacunarity-based features were computed using a sliding box varying from 2 to 25 pixels.

Acharya et al. [44] present a study with 50 IR breast images (25 normal and 25 cancerous). They extract from the images a set of 16 texture features: homogeneity, energy, entropy, first to forth moments computed for the co-occurrence matrix, angular second moment, contrast, mean, short runs emphasis, long runs emphasis, grey level of non-uniformity, and the run percentage from the run length matrix. But, only four features: first moment, third moment, run percentage and grey level non-uniformity, were selected as they were clinically significant compared to the other features.

Kapoor and Prasad [33] use statistical parameters such as skewness and kurtosis as features. They state that the larger the tumour is, the larger it is the temperature variation. They use the cumulative histogram for representing the temperature variation with the area to reflect the asymmetry. However, no segmentation results are reported. In addition, neither they made any comments about their results on classification nor even compare their work with others.

Nurhayati et al. [81] use tabulated first order statistics features: mean, standard deviation, variance, entropy, skewness and kurtosis. In Nurhayati et al. [51] the first order statistics features are combined with principal component analysis (PCA) method. The authors plot each feature chosen by PCA technique with the mean or variance feature in graphics and present a clustering approach.

Tavakol et al. [82] made a comparison between contralateral breast images to find asymmetric temperature distribution. They use as feature the mutual information associated with nonparametric windows technique to enhance the resolution to a highly oversampled image. Their experiments were performed with 60 simulated breast thermal images. Results showed that the more similar the thermal images of right and left breasts are, the closer it is the normalized mutual information value to one.

Zadeh et al. [74] use a set of 120 patients to extract four features: average, variance, skewness and kurtosis.

Resmini [53] had used images from patients with breast cancer, benign tumour, and with no diseases. Images were segmented and divided in four quadrants of equal size. Each quadrant presents a given number of pixels. Non breast regions are removed of the analyses. The methodology proposed extracted a total of 712 features divided in three groups. First group had used 32 features based on simple statistical measure: average, standard deviation, range between minimum and maximum tone of grey scale pixel and the area of last bin in a posterization on ten bins. Second group had used Higuchi Fractal Dimension as feature extractor, and provide total

Table 4
Summary of the feature extraction.

Paper	Feature extraction	Evaluation criteria	Comparison	Special characteristics
Lipari and Head [66]	Mean, median, standard deviation, maximum and minimum value of temperature for each mama and each quadrant	Not specified	Not specified	Not specified
Kuruganti and Qi [27]	Means, variance, skewness, and kurtosis, the peak pixel intensity of the correlated image, entropy and joint entropy	Correlation measure to asymmetric analysis	Not specified	Not specified
Koay et al. [48]	Mean, standard deviation, median, maximum, minimum, skewness, kurtosis, entropy, area and heat content	Artificial neural network (ANN) with back propagation	Not specified	At end, they use just two features: mean and standard deviation
Ng and Kee [43]	Mean, mode, points of temperature, median and biological data of patient	ANN, RNFN	Human specialist evaluation	Linear regression and correlation
Arora et al. [32]	Proprietary System	Three way: screening, clinical and ANN	Biopsy	Not specified
Qi et al. [69]	Histogram, mean, variance, skewness, kurtosis, correlation, entropy and joint entropy	*k*-means and *k*-nearest-neighbourhood	Not specified	Not specified
Tang et al. [49]	Local temperature increase amplitude by morphological signal processing	Not specified	Not specified	Not specified
Wiecek et al. [76]	Mean, standard deviation, variance, skewness, kurtosis, energy, variance, difference variance, correlation, inverse difference and entropy	ANN	Not specified	Not specified
Schaefer et al. [72,77]	Basic statistical features, moments, histogram features, cross co-occurrence matrix, mutual information, and Fourier analysis	Fuzzy rule-based classification system	Compares outcomes of accuracy with other examination modalities as mammogram and MRI	Not specified
Silveira Filho et al. [59]	Lacunarity measure	Graphic with the straight obtained for each breast	Diagnosis by biopsy	Not specified
Serrano et al. [60] and Conci et al. [62,63]	Lacunarity measure and Hurst coefficient	Graphic with the straight obtained for each breast	Diagnosis by biopsy	Not specified
Nurhayati et al. [51,81]	Mean, variance, skewness, kurtosis, entropy	Graphics with features chosen by PCA technique	Not specified	Not specified
Acharya et al. [44]	Homogeneity, energy, entropy, 4 first moments, entropy, angular second moment, contrast, mean, short and long runs emphasis, run percentage, grey level and run length non-uniformity	Support vector machine (SVM)	Not specified	Three-fold stratified cross validation was used to test the SVM classifier. 36 images for training (18 normal and 18 malignant)
Kapoor and Prasad [33]	Temperature variation, skewness and kurtosis	Clusterization	Not specified	Not specified
Borchartt et al. [64]	Range of temperature, mean, standard deviation and the last bin of a quantization of ten bins	SVM	Diagnosis by biopsy	Not specified
Zadeh et al. [74]	Mean, variance, skewness and kurtosis	*k*-means and *c*-means	Not specified	Not specified
Wishart et al. [6]	Not specified	Four way: screening, clinical and two ANN	Biopsy and sentinel BreastScan results	Not specified

of 40 features. And third group had used 640 features based on geo-statistic measures: Moran index and Geary coefficient.

Borchartt et al. [64] extract some simpler statistical features from IR images: range (i.e., the difference between the pixels of greater and lesser intensity); mean intensity; standard deviation, to show the dispersion of ROI pixels intensity from the mean; and a feature called "quantization", which measures the area occupied by a bin with the higher grey scale in a posterization in eight bins. For classification the authors used 28 images, being 24 from patient with pathology and 4 from patients without any pathology. In other work, Borchartt et al. [54] combined the features proposed by Serrano et al. [60] and Borchartt et al. [64].

The main points of the above papers are compared in Table 4.

6. Classification and evaluation measures

A key step in pattern recognition techniques is the classification and evaluation of the measured features [83]. In the case of thermal images of the breast, this step is responsible for pointing out if the patient has a healthy or an unhealthy breast. As one could expect, in order to perform the classification it is necessary to use some decision techniques. The classification between healthy and unhealthy breast image is a binary classification problem. In this case, four possible cases are considered: *true positive* (TP), which correspond to diseased breast that is correctly classified as unhealthy; *false positive* (FP), where a healthy breast is incorrectly classified as unhealthy; *true negative* (TN), where a healthy breast is correctly classified as healthy; and *false negative* (FN), which corresponds to a diseased breast that is incorrectly identified as healthy. Using the obtained classification results (i.e., the number of images in each one of these four classes), the most common performance measures are [84]: $accuracy=(TP+TN)/(TP+FP+FN+TN)$, $precision=TP/(TP+FP)$, $sensitivity\ (or\ recall)=TP/(TP+FN)$, and $specificity=TN/(TN+FP)$. Trade-off measures are also often used. For example, the F1-score, that is, the harmonic mean between precision and sensitivity. Graphical tools allow comparing the performance of different classification algorithms. In particular, one of the most used representations is the Receiver Operating Characteristic (ROC) curve that displays TP rate against FP rate for different compared classifiers [83]. Most work on the analysis of breast thermal images provide classification results using the accuracy, specificity and sensitivity measures or/and also present the corresponding ROC curves of their methods [83].

Other essential aspect in any automatic image processing systems is pattern classification [84]. In this stage, a class or label is automatically assigned to each of the test patterns. In case of supervised classification, it is assumed that a collection of training patterns is given, and these consist in labelled patterns where their corresponding correct class is known and also given. With these learning patterns the classification system learns to generalize and it is able to classify non-labelled test patterns. Non-supervised classification assumes non-labelled training data and it aims to determine classes during learning stage in order to correctly classify new test patterns. Common supervised classification techniques applied to breast thermal image analysis are neural networks, like *multilayer perceptrons* (MLP) [85,86] or *radial basis function* (RBF) networks [87], and *support vector machines* (SVM) [44,64]. Among non-supervised techniques, the most common ones are clustering algorithms like the *k*-means method [88,74], and *self-organizing maps* (SOM) neural networks.

In many practical classification problems, the involved patterns present a high dimensionality (i.e., great number of features that describe the patterns). In these cases, it becomes necessary to map the high-dimensional data into a lower dimensional space that preserve as much as possible the information represented in the patterns. Data dimensionality reduction [89] is carried out before the classification stage. The data mapping can be linear, like in principal component analysis (PCA), linear discriminant analysis (LDA) and independent component analysis (ICA); or non-linear, like non-linear PCA and Kohonen maps.

Amo et al. [90] use fuzzy classifiers to assign degrees of membership (or soft labels) for a pattern to consider multiple classes and take decisions based on membership values. A fuzzy classification result can be de-fuzzified to produce crisp result. Fuzzy classification methods, and in particular rule-based fuzzy classifiers, present several advantages like: the handling of uncertainty along the classification process, to be more robust under errors in input data, the number of needed rules are much lower than in crisp systems and these systems are close to human reasoning. In this context, hybrid neurofuzzy systems [91], fuzzy *c*-means [88] and fuzzy rule-based approaches [77] have been mainly applied to analysis of breast thermal images.

Among the works that apply supervised methods on breast thermal image analysis, different types of artificial neural networks were used. Results using MLP are presented in Ng and Fok [85]. These authors report values of 61.5% for accuracy, 68.9% for sensitivity and around 40% of specificity. Using RBF networks for binary image classification, Ng et al. [87] report better results: 81.2% of sensitivity, 88.2% of specificity and 80.9% of accuracy results. SVM were used in Borchartt et al. [64] for breast disease diagnosis and their proposed method reported average results of 85.7% of accuracy, 95.8% of sensitivity and 25.0% of specificity. Acharya et al. [44] also applied SVM for automatic classification of images as normal and malignant breast conditions. Their system offers an accuracy of 88.1%, sensitivity of 85.7% and specificity of 90.4%.

Jakubowska et al. [86] applied two approaches for dimensionality reduction, PCA and LDA, respectively, to reduce the number of features computed after the application of a wavelet transform on breast thermal images. Later the dimensionality reduction, reduced-dimensional images are classified as healthy or pathological using a MLP neural network.

Koay et al. [48] described a configuration of artificial neural network (ANN) with Back Propagation (BP) that is unsuccessfully applied in the classification of the subset of five features. After reducing the subset of features to only two of them (mean temperature difference and standard deviation difference) an ANN using only one hidden node (1-1-1) reported only two false negative outcomes. According to theses authors, a possible explanation for the false negative outcomes is the small number of images of patients with cancer (just 19 images being 14 from normal diagnostic and 5 from abnormal diagnostic). In order to fully assess the ability of ANN to predict true outcomes based on statistical inputs, the authors claim that more patients should be recruited for the study [48].

The Fuzzy Adaptive Learning Control Network-Another Adaptive Resonance Theory (FALCON-AART) [91] is an example of hybrid fuzzy-neural system with good classification capabilities at reduced training times. FALCON-AART achieves an accuracy result of 90% for breast tumour detection, and accuracy of 93% when discriminating benign and malignant breast tumours.

In the Ng and Kee work [43] the classification was made using an ANN. Linear regression was applied in data and a RBF network was used to decide the diagnostic in pathologic case (i.e., cancer or benign tumour) or health patient. The validation of the proposed approach was performed using ROC curves. The authors reported precision of 80.95%, sensibility of 81.2% and specificity of 88.2%. Such values are much better than the typical ones achieved by human specialists, around 60 and 70%.

The method proposed by Tang et al. [49] considers that carcinomatous breast possibility is proportional to the maximum increment (or amplitude) of the suspicious focus region. They use morphological signal processing to determine these amplitude values and determine an optimal threshold for cancer detection from the ROC curve based on Youden's index maximization. Using this threshold the proposed approach achieved 93.6% of sensitivity and 55.7% of false positive rate for 47 malign cancer cases from a population of 117 breast disease patients.

Arora et al. [32] analysed 92 patients, of whom 58 have some malignant tumour and 34 some benign tumour. Each patient underwent three types of analysis, named by the authors as (i) screening, (ii) clinical, and (iii) by artificial neural network. In the first analysis the patients were ranked according the risk of breast cancer from zero (without risk) to seven (very high risk). In the clinical analysis the authors used mammography and ultrasound images to verify the assessment as positive or negative for pathology. The neural network-based analysis applied an artificial intelligence technique to identify the presence of a malignant tumour in the breast.

Wiecek et al. [76] classify the thermal images as "with tumour" or "without tumour". Their approach was evaluated using 30 images of healthy patients and 10 images of patients with malignant tumour. For each patient breast four thermograms were acquired with frontal and lateral views. The authors claim that they use an ANN to analyse the extracted features. However, they report results only for the average of the temperatures.

In Schaefer et al. [72,77], the authors use a genetic algorithm to reduce to about 100 rules the original set of 2,812 rules of a neuro fuzzy system to classify breast thermal images. This reduced system is more time-efficient than the original one and it presented an acceptable classification accuracy result of 80.8%.

Delgado and Luna [39] used a preliminary diagnosis established according to thermo biological criteria (TH) proposed by Hobbins [92]: TH1—normal uniform non-vascular; TH2—normal uniform vascular; TH3—dubious; TH4—abnormal; or TH5—severely abnormal.

Boquete et al. [93] describe a method for automatic detection of the region with high risk of occurrence of a tumour finding in thermal images. They transform the pseudo-colour thermal breast image from RGB to the YCrCb colour space and apply the ICA dimensionality reduction method on each channel. In turn, the three ICA images are converted into binary images using Otsu's threshold [71] and a post-processing is applied to combine the outcomes and discriminate the tumour areas.

In Serrano et al. [60] the proposed feature vectors were processed by a machine learning software called WEKA [94], and as a result the given IR images are classified into "healthy" or "unhealthy". The ROC curve analysis shows that Naïve Bayes and Naïve Bayes Updateable present the best area under ROC curve of 0.958 using the standard deviation for right and left breasts.

Acharya et al. [44] train a support vector machine (SVM) [95] classifier. They apply cross-validation to discriminate between normal and malignant breast conditions. Their system produces an accuracy of 88.1%, sensitivity of 85.71% and specificity of 90.48%.

Resmini [53] uses a PCA technique to reduce dimension of sample, and sixteen features were chosen as the most significant ones. Classification was made by SVM implementation present on WEKA software. Results achieved show that features based on geo-statistic measures were particularly important to classify diagnosis. The methodology achieved 82.14% of accuracy, 91.7% of sensibility and 25% of specificity.

Zadeh et al. [74] apply two algorithms of clustering, namely *k*-means and *c*-means, for performing the classification of the patients as cancerous or non-cancerous. The authors do not show their results in terms of specificity, sensitivity or accuracy.

In Borchartt et al. [64] a LibSVM classifier [96] with the leave-one-out technique was used in the classification procedure. The two classification approaches described differ by extracting features from the entire ROI (first approach), and from the quadrants of the ROI (second approach). Results show that the first approach is more suitable for the used features, where the authors achieved 85.71% of accuracy, 95.83% of sensibility and 25% of specificity. The second approach presented 60.7% of accuracy, 66.7% of sensitivity and 25% of specificity. The main drawback of these approaches is low specificity. The authors claim that this could be related to the unbalance of the samples used in computation. Borchartt et al. [54] use a machine learning techniques available in WEKA and LibSVM software to classify the patient in "unhealthy" or "healthy". The proposed approach can

correctly classify the images up to 95% of the cases by using the Naïve Bayes classifiers and the standard deviation of a subtracted image of the patient breasts using the Hurst coefficient computed assuming different window sizes.

7. Image interpretation for diagnosis assistance

Computer Aided Diagnosis (CAD) systems for medical imaging provides complementary tools to help doctors on the interpretation of exams. Like in other scientific disciplines, the availability of better computer systems and more advanced classification algorithms has made possible a significant advance in the accuracy of CAD systems for medical applications in last decades. In particular, for the case of breast thermal images, the need of automatic thermographic interpreters was pointed out since the late 1970s [97].

To improve the performance of CAD systems for breast cancer image-based diagnosis, it is necessary to reduce the semantic gap between the high-level medical concepts (which are described linguistically) and the low-level information present in computer images (i.e., the image pixels). An intermediate semantic level can be provided by the use of medical ontologies. This field of Artificial Intelligence aims to produce formal representations of a set of concepts within a domain and to formally define the relationships between these concepts [98]. Ontology languages are used to encode the ontologies. Several attempts have been produced to apply ontology principles to breast histopathology image analysis [99] and also to mammography images [56]. Such mammographic ontology is based on the BIRADS [100] and allows to formally describe some types of abnormalities to define the properties (or features) and relations among these abnormalities. Tutac et al. [99] use Ontology Web Language standards [101] to translate the information contained in histological images to pathologist's domain for improving breast cancer grading results. However, there is still a lack of extending the application of medical ontologies to breast thermal images.

Negin et al. [97] implemented a basic software tool whose results demonstrated that the automatic interpreter outperformed from 4 to 7% the classification results produced by a human interpreter with respect to both thermographic impression and biopsy, considering the same test images.

More recently, different software tools have been proposed for breast thermal image processing. Arora et al. [32] perform a two-year study on New York Presbyterian Hospital-Cornell with 92 women for whom a breast biopsy had been recommended on the basis of a previously suspicious mammogram or ultrasound. The study assess the effectiveness of a digital infrared thermal image (DITI) system, the Sentinel BreastScan (Infrared Sciences Corp.) in detecting breast pathology in a group of patients with suspicious findings on either mammography or ultrasound that all underwent biopsy in a prospective, double-blinded trial. Ninety-four biopsies were analysed (60 malignant, and 34 benign) in women with ages ranging from 23 to 85. Their system considers 3 approaches to evaluation: (i) an overall risk score in the screening mode; (ii) a clinical score based on patient information; and (iii) an assessment by artificial neural network. Their report as result of 97% sensitivity, 44% specificity, and 82% negative predictive value depending on the mode used.

Wiecek et al. [76] described a tool developed in MATLAB that implements thermal signature calculations to detect pathological cases using first and second order statistical parameters computed from 2D wavelet transform of the image.

Umadevi et al. [102] developed the software called ITBIC for breast thermal image interpretation. Their system captures three thermal images for each female subject screened (i.e., frontal, left and right views) and then extracts highest temperature area of the thermograms and creates a simplified image for its interpretation. The authors reported the following results provided by the IBTIC interpreter on 50 female breast thermal images: positive predictive value of 80%, negative predictive value of 95.6%, sensitivity of 66.7%, and specificity of 97.7%.

Wishart et al. [6] present a novel artificial intelligence programme called NoTouch BreastScan and compare their results with Arora et al. [32]. When Wishart et al. [6] repeat the experience of Arora et al. [32] using the Sentinel BreastScan, their results show a low sensitivity in both screening mode (53%) and neural network (48%) which does not concur with previously published data by Arora et al. [32]. The results achieved by NoTouch BreastScan are sensibility of 48% and specificity of 70%.

Moghbel and Mashohor [103] present a survey on CAD systems using thermography. They compare different approaches based on neural networks and fuzzy systems that have been implemented in different CAD designs. According to the authors, the greatest improvement in CAD systems was achieved with a combination of fuzzy logic and artificial neural networks in the FALCON-AART and complementary learning fuzzy neural network (CLFNN). With a CAD design based on FALCON-AART, it was possible to achieve an overall accuracy of near 90%. This confirms that CAD systems are indeed a valuable addition to the efforts for the diagnosis of breast cancer. The lower cost and high performance of new infrared systems combined with accurate CAD designs can promote the use of thermography in many breast cancer centres worldwide.

8. Computer modelling

Some complementary analysis can be performed using IR images, papers that discuss these are commented in this section. Thermal image is a two-dimensional (2D) map of temperature on three-dimensional (3D) positions of the breast surface. The main goal of any numerical simulation is to quantify the complex relationships between the breast thermal behaviours and the underlying physiological conditions. Numerical modelling of the heat transfer in a woman breast may reveals conditions under which tumours and others diseases can be detected by thermograms. It could consider the sensitivity of each parameter involved in this process. The breast

geometry representation is important in the attempt to find possible factors related to a valid of overall breast pathological diagnosis. In conjunction with IR images that representation can be used also to estimate some thermal physical properties of the breast. These are the aims of many works in breast geometric modelling. However, few works are dedicated to represent real geometries of patients on the representation of the breast in order to model and consequently to analyse a 3D tumorous breast.

Zhang, et al. [104] apply finite element analysis to study the effects of geometrical parameters of the tumour (such the location and size) in the thermal diagnosis conditions. To simplify the theoretical analysis, the breast is seen as a semi-sphere and the tumour is considered a sphere positioned in spherical coordinates. Their numerical results show that it is difficult to identify the tumour by using surface temperature expression when the tumour is more than 3 cm below the skin surface. The effect of the environmental temperature on the surface temperature expression is significant, but that of the surface convective heat transfer is not significant according their experiments. Various values of emissivity ranging from 0.9 to 1.0 are considered. Their results show that the distance between the surface and the tumour plays an important role to the surface temperature expression. Moreover, during the thermal diagnosis, the decrease of environmental temperature will promote the visibility, but the increase of surface convective heat transfer is not helpful.

Lin et al. [105] present a 3D finite element breast model to investigate the relationship between an embedded tumour and surface temperature distribution. They present techniques to enhance the thermal signature of breast tumour that, as they stated, allow finding it (even in case of small tumour in deep regions). In their model, the breast is assumed to be hemispherical in shape and consist of four layers: skin, subcutaneous fat, glandular tissue and muscle core. It is completely regular and the areola is in the middle area of the skin layer. They use the Pennes bio-heat equation to calculate the influence of the body heat in the skin surface [28]. As modelled by the authors, the tumour is spherical and continuous grown is considered.

Jiang et al. [106] presents an inverse-problem modeling technique that considers and estimates the thermal profile of breast thermograms. The first modeling method is the Forward Thermography, which is based on the statistic Pennes equation [28], as well. The authors used the tetrahedron finite element (FE) meshing, to obtain the equation

$$\mathrm{KT} = P \tag{1}$$

where T is the unknown temperature vector, K is the thermal characteristic matrix of breast, and the vector P represents thermal loads. Finite-element model was applied in the quoted mesh in order to obtain the geometry of the breast. The second modeling method is the Inverse Thermography that objectifies the estimation of thermal properties in K and in P from T. But Eq. (1) has underdetermined nature, so spatial constraints were added to previous thermal properties, and the inverse thermal finite element method modeling equation was simplified.

Jiang et al. [107] present a 3D finite element method (FEM) based on thermal and elastic modeling techniques to improve the thermography potential as a reliable breast cancer detector. The method focuses on thermal and on elastic properties of both normal and tumorous breasts tissues. It considers that the presence of cancer provides temperature alteration and metabolic changes in the breast tissue. The method was applied to obtain the breast tissue geometry from a simple hemispherical model composed of four concentric tissue layers. Then, the generated model has gone through a progressive deformation due to application of the elastic model. Thermal equilibrium equation was used with FEM (under influence of steady-state Pennes equation) in order to ascertain temperature distribution of the breast. Galerkin approach [108] is used to derivate FE equations, enabling this equation being expressed as a thermal FE equation and establishing the static thermal FE modeling. A recursive finite difference method (FDM) was used in the discretization in the time domain for the dynamic thermal modeling, which is related to the heat conduction, blood perfusion and metabolic generation. Linear elastic FE modeling was obtained by the use of an elastic FEM technique in purpose of approximating the gravity-induced deformation in the breasts tissues. It was observed that breast tissue elastic properties have nonlinear behavior in case of huge deformations. So, the model proposed by Wellman [109] was chosen for the implementation of nonlinear elastic modeling. Furthermore, based on Azar et al. [110], it was developed an iterative pseudo-nonlinear scheme in order to obtain nonlinear elastic deformations of the breast by a series of step-wise linear approximations. In order to assess the correlation between the temperature distribution in the breast and the gravity-induced breast deformation under the influence of elastic properties, the static and dynamic thermal FE modeling methods were combined with the elastic FEM.

Santos et al. [111] conduct numerical simulations for a breast that presents a tumour, considering different tumour sizes and varying the tumour position inside the breast. A parametric analysis is performed and the results showed that the superficial temperatures became smaller as the tumour radius diminishes. This fact is an indicator that the detection of small tumours is difficult. Simulations with different tumour sizes located at different depths from the surface are performed as well. The results state that the superficial temperature of the breast presents an alteration in its value as the tumour size varies. From these, the authors concluded that both the tumour depth and its size are important sensitivity parameter on the temperatures profiles. Moreover, the results pointed out that the tumour depth is inversely proportional to the increase in temperature at the surface.

Silva [112] represents the real breast shape from 3 infrared images of a patient. From a database of 2D thermal images, curves are extracted and combined to generate a 3D model of the patient. This model has several important applications such as mesh generation for use in numerical methods for analysis and visualization. Such technique could be used in breast reconstruction or for definition of

the best prosthesis for the patient and to aid the diagnosis. A frontal IR image and two lateral ones are used to detect the body limit points in order to guide the geometric reconstruction of the shape. The obtained 3-dimensional geometrical mesh is verified by comparing it with photographic and 3D laser scan images.

Modelling the 3D geometry and the use of IR images for the reconstruction of the breast geometry were explored by Viana et al. [46] and Lima et al. [113]. First of all, an algorithm detects the contour of the body using threshold, and keeps these points in separated lists of coordinates. Limiting curves defining the breast contour to be modelled are obtained from frontal and lateral IR views. Curves are fitted using the least-square method. Some external prostheses were measured by a Coordinate Measuring Machine and the method allows choose among them, the one that best fit the patient original breast, on terms of size. The coordinates of the chosen prosthesis are used to tessellate a geometric mesh for numerical modelling in heat transfer analysis. The commercial software Fluent [114] was used to perform calculations of the temperature profiles. The following boundary conditions are considered: the heat exchange by convection among: the surface of the breast, the external environment (at 27.5 °C) and the breast (around 37 °C). The coefficient of convective heat transfer of 13.5 W/m^{2}C was adopted. Finally, the maximum temperatures obtained in the calculations are compared with that from the IR images of three patients with different pathologies. All of them have the clinical diagnosis and the most complete set of examinations using the right location of the nodule.

Amri et al. [37] studied the feasibility and limitations of the use of a transmission line matrix (TLM) on modelling and analysing a 3D tumorous breast. The TLM is a numerical technique for electromagnetics, mass and heat transfer. The authors also present a review of some previous works since the late 1970s. In that paper, the modelling of the bioheat equation is done with the help of Pennes equation [28,29]. The authors created a 3D regular breast model with a thermography device, consisting of multi-array IR sensors interfaced and a computer. The model of breast tumour is assumed to be spherical with many different diameters and depths. Their results pointed to importance of some thermography properties, like the influence of perfusion rate and heat transfer of a tissue in the steady-state temperature at the surface of this tissue.

Umadevi et al. [115] perform an experiment to estimate tumour parameters such as size and depth. They developed a framework called Infrared Thermography Based Image Construction (ITBIC) to estimate the tumour contour from the breast skin surface temperature. This framework first estimates the actual size and location of the tumour and, in turn, calculates depth using the Markov Chain Monte Carlo method. The authors validate the proposed method using two models: watermelon (a bulb is put on a phantom) and Agar (Agar powder was boiled in water around 30 min and poured into a plastic jar which contained electric bulb).

Grubisic et al. [116] present a 3D thermography system which is comprised by a 3D scanner and a thermal camera, leading to a more accurate and more representative representation of the modelled body. Their three-dimensional thermographic visualization can provide a better understanding of the body in analysis and diagnosis. The workflow has three steps: (i) calibration; (ii) acquisition; and (iii) medical applications, which leads to the construction of the three-dimensional thermogram. These components are controlled and synchronized by software running in a conventional PC. The 3D scanner is build using a video projector that emits structured light patterns on the object to be scanned, whilst the camera captures grey scale images of the projections generated by the emitted light. Thermal camera captures the thermal distribution on the surface of the object, generating thermograms that can be used for different purposes. The entire process encompasses the calibration of both 3D scanner and thermal camera. With this calibration process, the system is adjusted to start the acquisition process. Then, the 2D thermograms are associated with the 3D data generated by the scanner. The obtained results are 3D standardized thermograms representing the temperature distribution of the object (as a human breast). The results are shown on a special 3D visualization display. The evaluation methods are specified by the purpose of the analysis of the 3D thermogram. In their paper, the authors focused on the medical applications for the thermograms, especially regarding that the temperature distribution is intrinsically connected to biological or physiological processes related to some disease. In conclusion, there are three main kinds of medical applications: scientific modelling, scientific data analysis and scientific data visualization. Unfortunately, the authors do not provide details about the computing of the 3D mesh. A drawback of the proposed approach is the need to make each patient undergo a 3D scanning.

9. Conclusions

The thermography is non-invasive, radiation-free and complementary to anatomical investigations based on X-rays, ultrasound and three-dimensional scanning techniques such as CT and MRI [31,117]. Some works have been described in surveys as Kennedy et al. [118] and Sree et al. [119], where articles about breast thermal images are analysed and compared with other types of screening examination (clinical breast exam, mammogram, ultrasound, etc.). Currently the unique examination that provides 100% sure of the presence of a tumour is the biopsy. However, since the late seventies works show that thermography can aid on diagnosis especially when combined with other types of breast examination. The Ville Marie studies cited by Kennedy et al. [118] showed that thermography had a sensitivity of only 83% in detecting breast cancer, while the combination of mammography and thermography had a sensitivity of 95%. Although the review of all these works point credibility to the thermography, the IR imaging cannot be considered as a substitute for any other examination. However, it should be considered a complementary modality of breast disease detection. IR imaging can improve the sensitivity of breast cancer detection by capturing abnormalities in early and

even in non-palpable stages [3]. IR is also important because it is a practical and safe modality of imaging. Especially when combined with other types of examinations it may increase the possibilities of screening and could be a powerful tool for breast cancer detection. Therefore, research works on this subject are important in order to develop the ideal way to use this kind of resource. This development may include the definition of protocols of patient's image acquisition, training of the involved specialists, development of specialized CAD systems, and deployment of public image databases. The future of computer vision tools for breast cancer detection relies on the ability to qualify and to quantify changes in the metabolic behaviour of a patient by using pattern recognition techniques. Moreover, we can focus on the important fact that a unique type of image modality does not have power to detect all kinds of diseases, and consequently, any modality is not totally reliable in a broad range of infirmity. Certainly, in order to achieve the best diagnosis, to be able to detect the most diverse diseases, data from all related kinds of examinations should be integrated.

The aim of screening for any disease is to reduce mortality (and morbidity) from this disease by performing a test on an asymptomatic population, to detect disease at an earlier stage. For such purpose, IR images are very adequate. However, they are much more effectively used in combination with some other systems helping on the diagnosis and allowing it to be performed also by trained nurses or infrared thermography practitioners [5]. Criteria for assessing the validity of screening programs include that the screening test must be reliable, valid, and repeatable; must be acceptable, safe and easy to be performed; have a high positive predictive value; and be sensitive and specific. Furthermore, the screening program's cost should be evaluated with the benefits of early detection, and there should be an available effective treatment for managing the abnormality identified by the screening test. These criteria highlight necessary outcomes for studies of the effectiveness of infrared thermography in the domain of breast cancer screening and have suggested that thermograms should not be used alone as a method of screening, or as a replacement for mammography, but rather it should be used and evaluated as a complementary screening and detection procedure adjunctive to physical examination and mammography [42,120,121]. It is very high false positive rates potentially may present psychological costs (i.e., anxiety and confusion) that may be caused by receiving conflicting screening test results were also considered as relevant factors for adjunctive testing in breast cancer screening. The International Academy of Clinical Thermology [122] proposes that thermography can act as an "early warning" system by identifying signs of possible cancer or precancerous cell growth that would not be detectable by other screening methods for up to ten years. In screening programme this could be of great advantage. Evaluating the use of thermography in a cancer detection program, or as being part of a multimodal-screening programme, was not within the scope of this review [42].

A significant finding of the reviews conducted on this work is that there is no universally accepted systematic approach for acquisition and publication of results on infrared imaging. Most of the published studies on thermography refer to images that are no longer available. We believe that the major gaps in knowledge at this time can only be addressed by large-scale and systematic acquisition. Therefore, one major flaw identified by this survey is that there is no a protocol or a standardization to support the clinical effectiveness and benefits that may occur from the complementary diagnostic use of thermography in clinical decision-making. An equally important finding is that there is no papers that examined all aspects involved in the use of IR as a possible issue on pattern recognition systems or computer vision for diagnostic setting.

Acknowledgements

This research was supported by the Brazilian CAPES projects: Pro Engenharias 021/2009 and Pro Cad NF 540/2009. The authors thank the anonymous reviewers for their suggestions, particularly the recommended references. The author A. Sanchez wants to thank to the Spanish Government MICINN projects TIN2008-06890-C02-02 and TIN2011-29827-C02-01.

References

[1] H. Usuki, Y. Onoda, S. Kawasaki, T. Misumi, M. Murakami, S. Komatsubara, S. Teramoto, Relationship between thermographic observations of breast tumors and the DNA indices obtained by flow cytometry, Biomedical Thermology 10 (4) (1990) 282–285.
[2] W.C. Amalu, W.B. Hobbins, J.F. Head, and R.L. Elliot, (2006) Infrared Imaging of the Breast—An Over View, In: The Biomedical Engineering Handbook, third edition, vol. Medical Devices and Systems, Chapter 25, CRC Press, pp 25.1–25.21.
[3] H. Usuki, T. Ikeda, Y. Igarashi, I. Takahashi, A. Fukami, T. Yokoe, H. Sonoo, K. Asaishi, What kinds of non-palpable breast cancer can be detected by thermography? Biomedical Thermology 18 (4) (1998) 8–12.
[4] J.F. Head, R.L. Elliott, Infrared imaging: making progress in fulfilling its medical promise, IEEE Engineering in Medicine and Biology Magazine 21 (2002) 80–85.
[5] A. Tejerina, Aula de Habilidades y Simulacíon em Patología de la Mama' (in Spanish), ADEMAS Comunicacíon Gráfica, Madrid, Spain, 2009 2009.
[6] G.C. Wishart, M. Campisid, M. Boswella, D. Chapmana, V. Shackletona, S. Iddlesa, A. Halletta, P.D. Britton, The accuracy of digital infrared imaging for breast cancer detection in women undergoing breast biopsy, European Journal of Surgical Oncology 36 (6) (2010) 535–540.
[7] J.R. Keyserlingk, P.D. Ahlgren, E. Yu, N. Belliveau, M. Yassa, Functional infrared imaging of the breast, IEEE Engineering in Medicine and Biology Magazine 19 (3) (2000) 30–41.
[8] E.Y.K. Ng, A review of thermography as promising noninvasive detection modality for breast tumor, International Journal of Thermal Sciences 48 (1) (2009) 849–859.
[9] N. Weidner, J. Folkman, F. Pozza, P. Bevilacqua, E.N. Allred, D.H. Moore, S. Meli, G. Gasparini, Tumor angiogenesis: a new significant and independent prognostic indicator in early-stage breast carcinoma, Journal of the National Cancer Institute 84 (24) (1992) 1875–1887.
[10] E.Y.K. Ng, N.M. Sudharsan, Effect of blood flow, tumor and cold stress in a female breast: a novel time-accurate computer simulation, Proceedings of the Institution of Mechanical Engineering in Medicine 215 (4) (2001) 392–404.
[11] E.Y.K. Ng, N.M. Sudarshan, Numerical computation as a tool to aid thermographic interpretation, Journal of Medical Engineering and Technology 25 (2) (2001) 53–60.
[12] P.M. Arabi, S. Muttan, and R.J. Suji, (2010) Image enhancement for detection of early breast carcinoma by external irradiation,

International Conference. on Computing Communication and Networking Technologies (ICCCNT), pp. 01–09.
[13] V. Agostini, M. Knaflitz, F. Molinari, Motion artifact reduction in breast dynamic infrared imaging, IEEE Transaction on Biomedical Engineering 56 (3) (2009) 903–906.
[14] B.F. Jones, A reappraisal of the use of infrared thermal image analysis in medicine, IEEE Transactions on Medical Imaging 17 (6) (1998) 1019–1027.
[15] L. Boltzmann, Ableitung des Stefan'schen gesetzes, betreffend die abhängigkeit der wärmestrahlung von der temperatur aus der electromagnetischen lichttheorie, Annalen der Physik und Chemie 258 (6) (1884) 291–294.
[16] A. Levy, A. Dayan, M. Ben-David, I. Gannot, A new thermography-based approach to early detection of cancer utilizing magnetic nanoparticles theory simulation and in vitro validation, Nanomedicine: NBM 6 (2010) 786–796.
[17] M.A. Fauci, R. Breiterb, W. Cabanskib, W. Fickb, R. Kochb, J. Zieglerb, S.D. Gunapalac, Medical infrared imaging—differentiating facts from fiction, and the impact of high precision quantum well infrared photodetector camera systems, and other factors, in its re-emergence, Infrared Physics and Technology 42 (3–5) (2001) 337–344.
[18] L.J. Ignarro, R.G. Harbison, K.S. Wood, P.J. Kadowitz, Dissimilarities between methylene blue and cyanide on relaxation and cyclic GMP formation in endothelium-intact intrapulmonary artery caused by nitrogen oxide-containing vasodilators and acetylcholine, Journal of Pharmacology Experimental Therapeutics 236 (1) (1986) 30–36.
[19] M. Anbar, L. Milescu, A. Naumov, C. Brown, T. Button, C. Carty, K. Al Dulaimi, Detection of cancerous breasts by dynamic area telethermometry, IEEE Engineering in Medicine and Biology Magazine 20 (1) (2001) 80–91.
[20] P. Gamagami., Indirect Signs of Breast Cancer: Angiogenesis Study, Atlas of Mammography, Blackwell Science, Cambridge, MA, 1996, pp. 231–258.
[21] M. Anbar, Hyperthermia of the cancerous breast—analysis of mechanism, Cancer Letters 84 (1) (1994) 23–29.
[22] E.Y.K. Ng, L.N. Ung, F.C. Ng, L.S.J. Sim, Statistical analysis of healthy and malignant breast thermography, Journal of Medical Engineering and Technology 25 (6) (2001) 253–263.
[23] H. Usuki, K. Ishimura, M. Hagiike, K. Okano, K. Izuishi, Y. Karasawa, F. Goda, H. Maeta, Thermographic examination for carcinoma, Biomedical Thermology 21 (4) (2002) 1–7.
[24] H. Qi, P.T. Kuruganti and W.E. Snyder, (2006) Detecting Breast Cancer from Thermal Infrared Images by Asymmetry Analysis, In: The Biomedical Engineering Handbook, third edition, vol. Medical Devices and Systems, Chapter 27, CRC Press, pp. 27.1–27.14.
[25] H. Qi and N. A. Diakides, (2003) Thermal infrared imaging in early breast cancer detection—a survey of recent research, 25th Annual International Conference of the IEEE EMBS, Mexico, pp. 1109–1112.
[26] H. Qi, N.A. Diakides, Thermal infrared imaging in early breast cancer detection, Augmented Vision Perception in Infrared, Advances in Pattern Recognition II (2009) 139–152.
[27] P.T. Kuruganti and H. Qi, (2002) Asymmetry analysis in breast cancer detection using thermal infrared images, Proceedings of Second Joint EMBS/BMES Conference, Houston, TX, USA, 2, 1, 1129–1130.
[28] H.H. Pennes, Analysis of tissue and arterial blood temperature in the resting human forearm, Journal of Applied Physiology 1 (1) (1948) 93–122.
[29] E.H. Wissler, Pennes' 1948 paper revisited, Journal of Applied Physiology 85 (1) (1998) 35–41.
[30] W.H. Land Jr., E.A. Verheggen, Multiclass primal support vector machines for breast density classification, International Journal of Computational Biology and Drug Design 2 (1) (2009) 21–57.
[31] B.F. Jones, P. Plassmann, Digital infrared thermal imaging of human skin, IEEE Engineering in Medicine and Biology Magazine 21 (6) (2002) 41–48.
[32] N. Arora, D. Martins, D. Ruggerio, E. Tousimis, A.J. Swistel, M.P. Osborne, R.M. Simmons, Effectiveness of a noninvasive digital infrared thermal imaging system in the detection of breast cancer, The American Journal of Surgery 196 (4) (2008) 523–526.
[33] P. Kapoor and S.V.A.V. Prasad, (2010) Image processing for early diagnosis of breast cancer using infrared images, 2nd International Conference on Computer and Automation Engineering, vol. 3, 1, pp. 564–566.
[34] M.C. Araújo, R.C.F. Lima, F. Santos, Desenvolvimento de um banco de dados como ferramenta auxiliar na detecção precoce de câncer de mama' 30° Iberian-Latin-American Congress on Computational Methods in Engineering, 1, Armação dos Búzios, RJ, Brazil, 2009 1–15.
[35] L.S. Motta, Obtenção Automática da Região de Interesse em Termogramas Frontais da Mama Para o Auxílio à Detecção Precoce de Doenças, M.Sc Dissertation (in Portuguese), Computer Institute, UFF, Niteroi, Brazil, 2010.
[36] PROENG, (2012) Image processing and image analyses applied to mastology, available at: 〈http://visual.ic.uff.br/en/proeng/〉, accessed in: 31 January 2012.
[37] A. Amri, A. Saidane, S. Pulko, Thermal analysis of a three-dimensional breast model with embedded tumour using the transmission line matrix (TLM) method, Computers in Biology and Medicine 41 (1) (2011) 76–86.
[38] S. Antonini, D. Kolaric, I.A. Nola, Z. Herceg, V. Ramljak, T. Kulis, J.K. Holjevac and Z. Ferencic, (2011) Thermography surveillance after breast conserving surgery—three cases, 53rd International Symposium ELMAR, Croatia, pp. 317–319, 14–16 September, 2011.
[39] F.G. Delgado, J.G.V. Luna, Feasibility of new-generation infrared screening for breast cancer in rural communities, US Obstetrics and Gynecology, Touch Briefings 5 (2010) 52–56.
[40] M. Kontos, R. Wilson, I. Fentiman, Digital infrared thermal imaging (DITI) of breast lesions: sensitivity and specificity of detection of primary breast cancers, Clinical Radiology 66 (2011) (2011) 536–539.
[41] American College of Clinical Thermology (ACCT) Breast Screening Procedure, Available in: 〈http://www.thermologyonline.org/Breast/breast_thermography_procedure.htm〉, accessed in 31 January 2012.
[42] J. Kerr, (2004) Review of the effectiveness of infrared thermal imaging (thermography) for population screening and diagnostic testing of breast cancer, NZHTA Tech. Brief Series. vol. 3, no. 3, Division of Health Sciences, University of Otago, New Zealand, July 2004.
[43] E.Y.K. Ng, E.C. Kee, Integrative computer-aided diagnostic with breast thermogram, Journal of Mechanics in Medicine and Biology 7 (1) (2007) 1–10.
[44] U.R. Acharya, E.Y.K. Ng, J.H. Tan, S.V. Sree, Thermography based breast cancer detection using texture features and support vector machine, Journal of Medical Systems (2010) 01–08.
[45] L.A. Bezerra, (2007) Uso de imagens termográficas em tumores mamários para validação de simulação computacional M.Sc. Dissertation (in Portuguese), Department of Mechanical Engineering, Federal University of Pernambuco, Brazil.
[46] M.J.A. Viana, R.C.F. Lima, T.L. Rolim, A. Conci, S. Silva, S. Francisco and G.S. Santos, (2010) Simulating breast temperature profiles through substitute geometries from breast prostheses, Proceedings of 17th International Conference on Systems, Signals and Image Processing, Rio de Janeiro, RJ, Brazil, pp. 304–307.
[47] L.S. Motta, A. Conci, R.C.F. Lima and E.M. Diniz, (2010) Automatic segmentation on thermograms in order to aid diagnosis and 2D modeling, Proceedings of 10th Workshop em Informática Médica, Belo Horizonte, MG, Brazil, vol. 1, pp. 1610–1619. Available in: 〈http://www.visual.ic.uff.br/proeng〉, accessed: 27 January 2012.
[48] J. Koay, C. Herry, M. Frize, Analysis of breast thermography with an artificial neural network, Engineering in Medicine and Biology Society—IEMBS 1 (1) (2004) 1159–1162.
[49] X. Tang, H. Ding, Y. Yuan, Q. Wang, Morphological measurement of localized temperature increase amplitudes in breast infrared thermograms and its clinical application, Biomedical Signal Processing and Control 3 (1) (2008) 312–318.
[50] Z.Q. Liu and C. Wang, Inventors, Method and Apparatus for Thermal Radiation Imaging, United States Patent, US006023637A, 8 February 2000.
[51] O.D. Nurhayati, A. Susanto, T.S. Widodo, M. Tjokronagoro, Principal component analysis combined with first order statistical method for breast thermal images classification, International Journal of Computer Science and Technology 2 (2) (2011) 12–18.
[52] Meditherm, (2012) The Meditherm med200, Available at: 〈http://www.meditherm.com/mms_default.htm〉, accessed in: 31 January 2012.
[53] R. Resmini, Análise de Imagens Térmicas da Mama usando Descritores de Textura, M.Sc. Dissertation (in Portuguese), Computer Institute, UFF, Niteroi, Brazil, 2011.
[54] T.B. Borchartt, R. Resmini, L.S. Motta, E.W.G. Clua, A. Conci, M.J.A. Viana, L.C. Santos, R.C.F. Lima and A. Sanchez, (2012) Combining approaches for early diagnosis of breast diseases using thermal

imaging', to appear in International Journal of Innovative Computing and Applications, Vol. and No. not released yet.
[55] Flir Systems (2004) ThermaCAM TM S45 Infrared Camera, User Manual, available at 〈http://yellotec.com/pdf/S45_Datasheet.pdf〉, accessed: January 13, 2012.
[56] H. Qi, (2002) Breast cancer identification through shape analysis in thermal texture maps, Proceedings of Second Joint EMBS/BMES Conference, Houston, TX, USA, vol. 2, pp. 1155–1156.
[57] Ville Marie Medical Center, Available at: 〈http://www.villemariemed.com〉, accessed in: 31 January 2012.
[58] BioBD, (2012) Banco de Dados de Pesquisa Biomédica, available at: 〈http://150.161.110.168/termo〉, accessed in: 31 January 2012.
[59] O.T. Silveira Filho, A. Conci, R. Carvalho, R. Mello, R.F.C. Lima, (2009) On using lacunarity for diagnosis of breast diseases considering thermal images, Proceedings of 16th International Conference on Systems, Signals and Image Processing, Chalkida, Greece, pp. 1–4.
[60] R.C. Serrano, J. Ulysses, S. Ribeiro and R.C.F. Lima, (2010) Using hurst coefficient and lacunarity to diagnosis early breast diseases, Proceedings of 17th International Conference on Systems, Signals and Image Processing, Rio de Janeiro, RJ, Brazil, pp. 550–553.
[61] A. Conci, R.C.F. Lima, C.A.P. Fontes, L.S. Motta, R. Resmini, A new method for automatic segmentation of the region of interest of thermographic breast image, Thermology International 20 (4) (2010) 134–135.
[62] A. Conci, R.C.F. Lima, C.A.P. Fontes, S.V. Silva, T.B. Borchartt, R. Resmini, On the breast reconstruction by thermal images, Thermology International 20 (4) (2010) 135.
[63] A. Conci, R.C.F. Lima, C.A.P. Fontes, T.B. Borchartt, R. Resmini, A new method to aid to the breast diagnosis using fractal geometry, Thermology International 20 (4) (2010) 135–136.
[64] T.B. Borchartt, R. Resmini, A. Conci, A. Martins, A.C. Silva, E.M. Diniz, A. Paiva and R.C.F. Lima, (2011) Thermal feature analysis to aid on breast disease diagnosis, Proceedings of 21st Brazilian Congress of Mechanical Engineering—COBEM2011, 24–28 October 2011, Natal, Brazil, pp. 1–8.
[65] Q. Zhou, Z. Li and J.K. Aggarwal, (2004) Boundary extraction in thermal images by edge map, Proceedings of the 2004 ACM Symposium on Applied Computing, pp. 254–258.
[66] C. Lipari and J. Head, (1997) Advanced infrared image processing for breast cancer risk assessment, Proceedings for 19th International Conference of the IEEE Engineering in Medicine and Biology Society, vol. 2, Chicago, 30 October to 2 November IEEE/EMBS, pp. 673–676.
[67] C.L. Herry and M. Frize, (2002) Digital processing techniques for the assessment of pain with infrared thermal imaging, Proceedings of the Second Joint EMBS/BMES Conference, Houston, TX, USA, vol. 2, pp. 1157–1158.
[68] N. Scales, C. Herry and M. Frize, (2004) Automated image segmentation for breast analysis using infrared images. Proceedings of the 26th Annual International Conference of the IEEE/EMBS, San Francisco, CA, USA, pp. 1737–1740.
[69] H. Qi, P.T. Kuruganti and W.E. Snyder, (2008) Detecting breast cancer from thermal infrared images by asymmetry analysis. In: N.A. Diakides and J.D. Bronzino, Medical Infrared Imaging, pp. 11.1–11.14.
[70] Z. Jin-Yu, C. Yan and H. Xian-Xiang, (2009) IR thermal image segmentation based on enhanced genetic algorithms and two-dimensional classes square error. Second International Conference on Information and Computation Science, vol. 2, no. 1, pp. 309–312.
[71] N. Otsu, A threshold selection method from gray-level histograms, IEEE Transactions on Systems, Man, and Cybernetics 9 (1) (1979) 62–66.
[72] G. Schaefer, M. Zavisek, T. Nakashima, Thermography based breast cancer analysis using statistical features and fuzzy classification, Pattern Recognition 42 (6) (2009) 1133–1137.
[73] R. Kafieh, H. Rabbani, Wavelet-based medical infrared image noise reduction using local model for signal and noise, IEEE Statistical Signal Processing Workshop (2011) 549–552.
[74] H.G. Zadeh, I.A. Kazerouni, J. Haddadnia, Distinguish breast cancer based on thermal features in infrared images, Canadian Journal on Image Processing and Computer Vision 2 (6) (2011) 54–58.
[75] G. Schaefer, S.Y. Zhu, B. Jones, An image retrieval approach for thermal medical images, Medical Image Understanding and Analysis (2004) 181–183.
[76] B. Wiecek, S. Zwolenik, A. Jung, and J. Zuber, (1999) Advanced thermal, visual and radiological image processing for clinical diagnostics', Proceedings of First Joint IEEE BMES/EMBS Conference, Atlanta, GA, USA, p. 1108.
[77] G. Schaefer, T. Nakashima, M. Zavisek, Analysis of breast thermograms based on statistical image features and hybrid fuzzy classification, LNCS 5538, Springer, 2008, pp. 753–762.
[78] C. Allain, M. Cloitre, Characterizing the lacunarity of random and deterministic fractal sets, Physical Review A 44 (6) (1991) 3552–3558.
[79] P. Dong, Lacunarity analysis of raster datasets and 1D, 2D, and 3D point patterns, Computers and Geosciences 35 (10) (2009) 2100–2110.
[80] A. Conci, R.C.F. Lima, R.C. Serrano, L.S. Motta and R.H.C. Mello, (2010d) Using fractal geometry to extract features of thermal images for early breast diseases, 14th International Conference on Geometry and Graphics, Kyoto, Japan, pp. 208–217.
[81] O.D. Nurhayati, T.S. Widodo, A. Susanto, M. Tjokronagoro, First order statistical feature for breast cancer detection using thermal images, World Academy of Science, Engineering and Technology (70) (2010) 1040–1042.
[82] M.E. Tavakol, E.Y.K. Ng, C. Lucas, S. Sadri, N. Gheissari, Estimating the mutual information between bilateral breast in thermograms using nonparametric windows, Journal of Medical Systems 35 (5) (2011) 959–967.
[83] S.H. Park, J.M. Goo, C.H. Jo, Receiver operating characteristic (ROC) curve: practical review for radiologists, Korean Journal of Radiology 5 (1) (2004) 11–18.
[84] R.O. Duda, P.E. Hart, D.G. Stork, Pattern Classification, second ed. Wiley, 2000.
[85] E.Y.K. Ng, S.C. Fok, A framework for early discovery of breast tumor using thermography with artificial neural network, The Breast Journal 9 (4) (2003) 341–343.
[86] T. Jakubowska, B. Wiecek, M. Wysocki, C. Drews-Peszynski and M. Strzelecki, (2004) Classification of breast thermal images using artificial neural networks, Proceedings of 26th Annual IEEE EMBS Conference, 1155–1158.
[87] E.Y.K Ng, E.C. Kee and R. Acharya, (2005) Advanced technique in breast thermography analysis, Proceedings of IEEE Conference on Engineering in Medicine and Biology, pp. 710–713.
[88] M.E. Tavakol, C. Lucas, S. Sadri, E.Y.K. Ng, Analysis of breast thermography using fractal dimension to establish possible difference between malignant and benign patterns, Journal of Health Care Engineering 1 (1) (2010) 27–43.
[89] L.J.P. van der Maaten, E.O. Postma, and H.J. van den Herik, (2009) Dimensionality Reduction: A Comparative Review, Tilburg University Technical Report, TiCC-TR 2009-005.
[90] A. del Amo, J. Montero and V. Cutello, (1999) On the principles of fuzzy classification, Proceedings of 18th North American Fuzzy Information Processing Society Annual Conference, 675–679.
[91] T.Z. Tan, C. Quek, G.S. Ng, E.Y.K. Ng, A novel cognitive interpretation of breast cancer thermography with complementary learning fuzzy neural memory structure, Expert Systems with Application 33 (3) (2007) 652–666.
[92] W.B. Hobbins, Abnormal thermogram—significance in breast cancer, Interamerican Journal of Radiology 12 (1987) 337.
[93] L. Boquete, S. Ortega, J.M.M. Jiménez, J.M.R. Ascariz, R. Blanco, Automated detection of breast cancer in thermal infrared images, based on independent component analysis, Journal of Medical Systems (2010) 1–9.
[94] M. Hall, E. Frank, G. Holmes, B. Pfahringer, P. Reutemann, I.H. Witten, The WEKA data mining software: an update, SIGKDD Explorations 11 (1) (2009) 10–18.
[95] R.E. Fan, P.E. Chen, C.J. Lin, Working set selection using the second order information for training SVM, Journal of Machine Learning Research 6 (2005) 1889–1918.
[96] C.C. Chang, C.J. Lin, LIBSVM: a library for support vector machines, ACM Transactions on Intelligent Systems and Technology 2 (3) (2001) 27.1–27.27.
[97] M. Negin, M.C. Ziskin, C. Piner, M.S. Lapayowker, A computerized breast thermographic interpreter, IEEE Transactions on Biomedical Engineering 24 (4) (1977) 347–352.
[98] S. Russell, P. Norvig, Artificial Intelligence: A Modern Approach, third ed. Prentice-Hall, 2010.
[99] A.E. Tutac, D. Racoceanu, T. Putti, X. Wei, L. Wee-Kheng, V. Cretu, Knowledge-guided semantic indexing of breast cancer histopathology images,, Proceedings of IEEE Internationnal Conference on Biomedical Engineering and Informatics (2008) 107–112.
[100] American College of Radiology (ACR) (2003) Breast Imaging Reporting and Data System Atlas (BI-RADS Atlas). Reston, VA: American College of Radiology.

[101] D.L. McGuiness and F. van Harmelen, (2004) OWL Web Ontology Language W3C Overview, available at: 〈http://www.w3.org/TR/owl-features/〉, accessed in: 13 January 2012.
[102] V. Umadevi, S.V. Raghavan and S. Jaipurka, (2010) Interpreter for breast thermogram characterization, IEEE EMBS Conference on Biomedical Engineering & Sciences (IECBES 2010), Kuala Lumpur, Malaysia, pp. 150–154.
[103] M. Moghbel, S. Mashohor, A review of computer assisted detection/diagnosis (CAD) in breast thermography for breast cancer detection, Artificial Intelligence Review (2011) 1–9.
[104] H. Zhang, L. He and L. Zhu, (2009) Critical Conditions for the thermal diagnosis of the breast cancer, 3rd International Conference on Bioinformatics and Biomedical Engineering, China, pp. 1–3.
[105] Q.Y. Lin, H.Q. Yang, S.S. Xie, Y.H. Wang, Z. Ye, S.Q. Chen, Detecting early breast tumour by finite element thermal analysis, Journal of Medical Engineering and Technology 33 (4) (2009) 274–280.
[106] L. Jiang, W. Zhan and M.H. Loew, (2010a) Modeling thermography of the tumorous human breast: from forward problem to inverse problem solving, 8th International Symposium on Biomedical Imaging, pp. 205–208.
[107] L. Jiang, W. Zhan, M.H. Loew, Modeling static and dynamic thermography of the human breast under elastic deformation, Physics in Medicine and Biology 56 (2010) 187–202.
[108] A. Ern, J.L. Guermond, Theory and Practice of Finite Elements, Springer, 2004.
[109] P.S. Wellman, Tactile Imaging, Harvard University, Cambridge, MA, 1999.
[110] F.S. Azar, D.N. Metaxas, M.D. Schnall, A deformation finite element model of the breast for predicting mechanical deformations under external perturbations, Academic Radiology 8 (1) (2001) 965–975.
[111] L.C. Santos, R.C.F. Lima, L. Bezerra, P. Lyra and A. Conci, (2010) Parametric analysis on the influences of tumour position and size in breast temperature profile, Proceedings of 17th International Conference on Systems, Signals and Image Processing, Rio de Janeiro, RJ, Brazil, pp. 478–481.
[112] S.V. Silva, (2010) Reconstrução da Geometria da Mama a partir de images termograficas, D. Sc. Thesis, UFF (in português).
[113] R.C.F. Lima, L.C. Coelho, M.J. Viana, S.V. Silva, M.C. Araújo, L.A. Bezerra, T.L. Rolim, E.D.C. Silva, P.R.M. Lyra, F.G.S. Santos, A. Conci, Uses of numerical simulation to find the best external breast prostheses and analyse the influence of tumor depth and tumor size in thermographic images, Thermology International 20 (4) (2010) 136.
[114] ANSYS Fluent, accessed in: 31 January 2012—available at: 〈http://www.ansys.com/Products/Simulation+Technology/Fluid+Dynamics/ANSYS+Fluent〉.
[115] V. Umadevi, S.V. Raghavan, S. Jaipurkar, Framework for estimating tumour parameters using thermal imaging, Indian Journal of Medical Research 134 (November) (2011) 725–731.
[116] I. Grubisic, L. Gjenero, T. Lipic, I. Sovic and T. Skala, (2011) Active 3D scanning based 3D thermography system and medical applications, MIPRO, 2011 Proceedings of the 34th International Convention on Information and Communication Technology, Electronics and Microelectronics, Opatija, Croatia, pp. 269–273.
[117] C.L. Vaughan, New developments in medical imaging to detect breast cancer, Continuing Medical Education 22 (3) (2011) 122–125.
[118] D.A. Kennedy, T. Lee, D. Seely, A comparative review of thermography as a breast cancer screening technique, Integrative Cancer Therapies 8 (1) (2009) 9–16.
[119] S.V. Sree, E.Y.K. Ng, R.U. Acharya, O. Faust, Breast imaging: a survey, World Journal of Clinical Oncology 2 (4) (2011) 171–178.
[120] International Academy of Clinical Thermology (IACT) (2012a), available in: 〈http://www.iact-org.org/〉, accessed 20 January 2012.
[121] N.A. Diakides, J.D. Bronzinho, Medical Infrared Imaging, USA, CRC Press, Boca Raton, 2008.
[122] International Academy of Clinical Thermology (IACT) (2012b), available in: 〈http://www.iact-org.org/patients/breastthermography/mammography-vs-therm.html〉, accessed 20 January 2012.